JOURNAL OF APPLIED ELECTROCHEMISTRY 15 (1985) 549–555

*Mass transfer at gas evolving electrodes**

L. J. J. JANSSEN, E. BARENDRECHT

Department of Chemistry, Laboratory for Electrochemistry, Eindhoven University of Technology, PO Box 513, 5600 MB Eindhoven, The Netherlands

Received 24 September 1984

A new convection–penetration model for mass transfer of indicator ions to a gas-evolving electrode with forced convection of solution is described theoretically. It has been found that the mass transfer of indicator ions to a gas-evolving electrode can be described well by the new model. The contribution of an oxygen bubble departing from the electrode surface to the mass transfer is much greater than the contribution of a departing hydrogen bubble.

Nonmenclature

a_d	proportionality factor
A_d	average cross-section of detached bubbles; bubble cross-section (m^2)
A_e	surface area of electrode (m^2)
c_i	concentration of species i in bulk solution (mol m^{-3})
d	bubble density of sites from which bubbles depart (m^{-2})
D_i	diffusion coefficient of species i (m^2 s^{-1})
E	electrode potential versus SCE (V)
F	Faraday constant, = 96.487 10^6 C $kmol^{-1}$
i	electric current density (kA m^{-2})
I	electric current (kA)
k_i	mass transfer coefficient of the indicator ion i (m s^{-1})
$k_{e,i}$	mass transfer coefficient of the indicator ion i obtained by extrapolation of k_i/i curve (m s^{-1})
$k_{f,i}$	mass transfer coefficient of the indicator ion i at forced convection in absence of gas bubble evolution (m s^{-1})
k'_i	mass transfer coefficient of the indicator ion i in convectionless conditions for the part of electrode surface from which a bubble had departed (m s^{-1})
$k'_{i,a}$	average value of k'_i for period t_d (m s^{-1})
$k'_{f,i}$	mass transfer coefficient of the indicator ion i at forced convection for the part of electrode surface from which a bubble had departed (m s^{-1})
$k'_{f,i,a}$	average value of $k'_{f,i}$ for period t_1 (m s^{-1})
k'_{f,i,a^*}	average value of $k'_{f,i}$ for period t_d (m s^{-1})
m_i	mass flux density of the indicator ion i (mol m^{-2} s)
N	number of detached bubbles per unit surface area and time (cm^{-2} s^{-1})
n	number of bubbles on a picture or on a part of a moving film (1)
n	number of electrons, involved in the reaction to form one molecule of a species (1)
p	a proportionality factor
R_d	average radius of departed bubbles; bubble radius (m)
$R_{d,i}$	radius of the departed bubble i (m)
$R_{d,m}$	maximum radius of departed bubble m (m)
$R_{S,d}$	Sauter bubble radius; $R_{S,d} = 3V_d/4A_d$ (m)
s	fraction of electrode surface coming into contact with fresh bulk electrolyte in period t_d (1)
t	time (s)
t_d	bubble cycle time (s)
t_1	time $D_i/\pi k^2_{f,i}$ (s)
T	temperature (K)
v_g	volumetric gas production rate (m s^{-1})
$v_{g,b}$	volumetric production rate of gas bubbles (m s^{-1})
v^0_g	volumetric production rate of gas bubbles

*Paper presented at the International Meeting on Electrolytic Bubbles organized by the Electrochemical Technology Group of the Society of Chemical Industry, and held at Imperial College, London, 13–14 September 1984.

0021–891X/85 $03.00 + .12

when all the gas is evolved as bubbles ($m\ s^{-1}$)
v_s solution flow velocity ($m\ s^{-1}$)
V_d average volume of departed bubbles; bubble volume (m^3)
V_M volume of 1 mol gas; 24.4×10^{-3} m^3 at 298 K($m^3\ mol^{-1}$)
η_g efficiency of gas bubble evolution (%)

Subscripts

a average value
b bubbles
d detached bubble
e electrode; extrapolated
f forced convection
fi ferricyanide ion
fo ferrocyanide ion
g gas
H hydrogen
i indicator ion i
m maximum
O oxygen
s solution

1. Introduction

The mass transfer of indicator ions to a gas-evolving electrode in natural convection has been thoroughly investigated and various mass transfer models are available [1–6]. However, only a few empirical correlations [7, 8] are available to calculate the mass transfer coefficient for a gas-evolving electrode with forced convection of bulk solution. The main purpose of this study is to present a model to predict the mass transfer of indicator ions to a gas-evolving electrode with superposition of hydrodynamic flow of the solution. The proposed model is a modification of the coalescence model given by Janssen and van Stralen [4].

2. Theory

The rate of mass transfer of indicator ions to a gas-evolving electrode is described by a new model in which only the detaching bubbles are taken into consideration. This means that the adhered bubbles have no influence upon the rate of mass transfer.

The formation, growth and detachment of a bubble on a site of the electrode surface requires a time t_d. On the same site this phenomenon is constantly repeated. When a bubble departs from a site on the electrode surface it is assumed that an electrode surface area $a_d A_d$ comes into contact with fresh bulk electrolyte having a bulk concentration of indicator ions, c_i, where A_d is the cross-section of a detached bubble and a_d is a constant factor. To calculate the mass transfer coefficient the following additional simplifications are made:

the radius, the cross-section and the volume of all detached bubbles are constant,

the distribution of the bubble-departure sites across the electrode surface is uniform,

the bubble cycle time, t_d, is equal for all electrode sites,

the detaching and rising bubbles induce no solution flow except the flow necessary for refreshment of solution at the electrode surface,

no effect of migration of indicator ions is considered.

From the rate of volumetric gas bubble formation per unit surface area, $v_{g,b}$, and the volume V_d of a detached bubble it follows that the number of detached bubbles per unit surface area and time is given by

$$N = v_{g,b}/V_d \tag{1}$$

Since the density of sites from which bubbles depart, d, is equal to Nt_d, the fraction of electrode surface coming into contact with fresh bulk electrolyte in a period t_d is given by

$$s = Nt_d a_d A_d \tag{2}$$

First, the effect of forced convection on the mass transfer coefficient is discussed separately for a bubble-free surface and then an electrode surface from which bubbles detach is treated.

For a bubble-free electrode surface under forced convection the mass transfer coefficient is given by $k_{f,i}$. Consequently, for the fraction $1 - s$ of the electrode surface not in contact with fresh bulk electrolyte the mass transfer coefficient is equal to $k_{f,i}$. For the fraction s of

electrode surface in contact with fresh bulk solution, the calculation of the average mass transfer coefficient is complicated. During the bubble cycle the mass transfer coefficient directly after bubble detachment is greater than $k_{f,i}$ and becomes equal to $k_{f,i}$ after a certain time t_1.

The solution in the diffusion layer is regarded as convectionless. From the well-known Cotrell relation it follows that for semi-infinite linear diffusion the mass transfer coefficient, k'_i, is given by

$$k'_i = D_i^{1/2}/\pi^{1/2}t^{1/2} \tag{3}$$

Since k'_i at t_1 is also equal to $k_{f,i}$, it can be shown that

$$t_1 = D_i/\pi k_{f,i}^2 \tag{4}$$

The bubble cycle time t_d is divided into two parts, namely, t_1 and $t_d - t_1$. For the fraction s of the electrode surface and assuming the bubble cycle time is greater than t_1, the mass transfer coefficient during time $t_d - t_1$ is given by $k_{f,i}$ and the average mass transfer coefficient during time t_1 by

$$k'_{f,i,a} = \frac{1}{t_1}\int_0^{t_1} k'_i \mathrm{d}t \tag{5}$$

By substitution of k'_i, using Equation 3, into Equation 5 and after integration it follows that

$$k'_{f,i,a} = 2D_i^{1/2}/\pi^{1/2}t_1^{1/2} \tag{6}$$

The mass transfer coefficient averaged over one bubble cycle is given by

$$k'_{f,i,a^*} = \frac{k'_{f,i,a}t_1 + k_{f,i}(t_d - t_1)}{t_d} \tag{7}$$

From Equations 4, 6 and 7 it is found that

$$k'_{f,i,a^*} = k_{f,i} + \frac{D_i}{\pi k_{f,i}t_d} \tag{8}$$

The total mass transfer coefficient for a gas-evolving electrode under forced convection is

$$k_i = k_{f,i}(1 - s) + k'_{f,i,a^*}s \tag{9}$$

From Equations 8 and 9 it follows that

$$k_i = k_{f,i} + \frac{D_i s}{\pi k_{f,i}t_d} \tag{10}$$

and from Equations 1, 2 and 9 that

$$k_i = k_{f,i} + \frac{D_i a_d A_d v_{g,b}}{\pi k_{f,i}V_d} \tag{11}$$

The first term of Equation 11 incorporates the mass transfer in forced convection and in the absence of gas bubble formation; the second term gives the contribution caused by detached bubbles.

3. Results

3.1. *Parameters characterizing the behaviour of bubbles and efficiency of gas bubble formation*

In order to characterize the bubble behaviour the following parameters have been determined from pictures of a certain region just above the top of the working electrode: radius of bubble i, $R_{d,i}$, average bubble radius, R_d, average bubble cross-section, A_d, average bubble volume, V_d, and Sauter bubble radius, $R_{S,d} = 3V_d/4A_d$. The experimental details are given in a paper by Janssen and Barendrecht [9].

For oxygen bubbles the Sauter bubble radius determined using high speed cine photography is shown as a function of current density i_O at various bulk solution flow velocities in Fig. 1. From high speed films also the volumetric rate $v_{g,b}$ of gas bubble evolution has been determined. From this rate and the theoretical one, namely, $v_g^0 = \mathrm{nFi_g}V_M$ where V_M is the volume of 1 mol of gas ($V_M = 24.4 \times 10^{-3}$ m^3 mol^{-1} at 298 K), the efficiency of gas bubble evolution $\eta_g = 100\, v_{g,b}/v_g^0$ is calculated.

In Fig. 1 η_g is presented as a function of current density i_O at various bulk solution flow velocities. The results of Fig. 1 are remarkable; only about one half of the oxygen formed is evolved in the form of bubbles and the rest is transported in the dissolved condition from the electrode surface.

For hydrogen bubbles the Sauter bubble radius is plotted as a function of current density i_H for a bulk solution flow velocity of 0.12 m s^{-1} in Fig. 2. This figure shows the efficiency of gas evolution as a function of current density i_H at $v_s = 0.12$ m s^{-1}. Taking into account the experimental inaccuracy, it is assumed that η_g is practically constant, namely, 75%, in the current density range from 0.05 to 1.0 kA m^{-2}. From Figs. 1 and 2 it follows that η_g for hydrogen is clearly higher than η_g for oxygen.

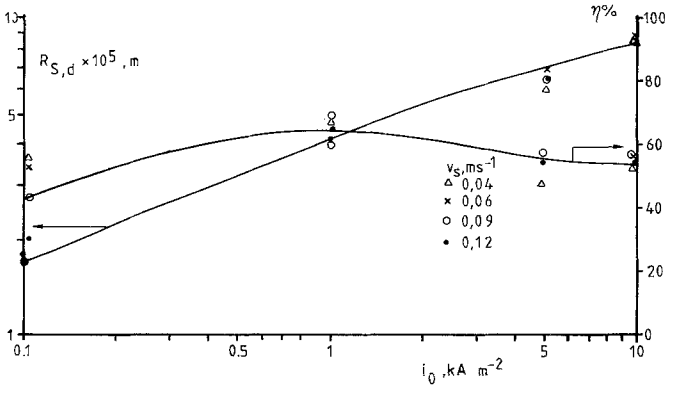

Fig. 1. Sauter bubble radius, $R_{S,d}$, and efficiency of gas bubble formation, η, both determined by the high speed film method, as a function of current density for oxygen evolution on a nickel electrode in 1 M KOH and at 298 K and various bulk solution flow velocities v_s.

3.2. *Mass transfer coefficient*

The redox couple $Fe(CN)_6^{3-}/Fe(CN)_6^{4-}$ is very useful in determining the mass transfer coefficient k_l for the hydrogen-evolving electrode at $i_H > \simeq 0\,mA\,cm^{-2}$ as well as for the oxygen-evolving electrode at $i_O > \simeq 10\,mA\,cm^{-2}$ [10], since under these conditions the concentration of the indicator ion at the surface of the gas-evolving electrode is practically zero. The mass transfer coefficient k_i of indicator ion i to a gas-evolving electrode is calculated with the well known equation

$$k_i = m_i/A_e c_i \qquad (12)$$

where m_i is the rate of oxidation or reduction of indicator ions, A_e is the electrode surface area and c_i is the concentration of the indicator ion in the bulk of the solution. In the calculation of k_i, the average concentration of the indicator ion during the experiment was used.

The current for formation of oxygen or hydrogen i_O or $i_H = i - i_i$ where i is the adjusted current density and i_i is the current density for the oxidation or reduction of indicator ions. The current density $i_i = nFm_i$.

3.2.1. Oxygen-evolving electrode. To determine the dependence of k_{fo} on i_O, mass transfer experiments were carried out over a wide range of current density, from 0.1 to 10 kA m^{-2}. It was found that $k_{fo} = k_{e,fo} + P_O i^{0.85}$ for v_s from 0.04 to 0.12 m s^{-1} and that $k_{e,fo}$ is higher than $k_{f,fo}$, where $k_{f,fo}$ is the mass transfer coefficient for $Fe(CN)_6^{4-}$ at forced convection and in the absence of gas evolution. Moreover, P_O decreases with increasing v_s.

The mass transfer coefficient k_{fo} is given in Fig. 3 as a function of $i_O^{0.85}$ for an oxygen-evolving nickel electrode in 1 M KOH as the supporting electrolyte, at 298 K and various v_s. Linear extrapolation of a $k_{fo}/i_O^{0.85}$ curve gives k_{fo} at $i_O = 0\,kA\,m^{-2}$, denoted by $k_{e,fo}$.

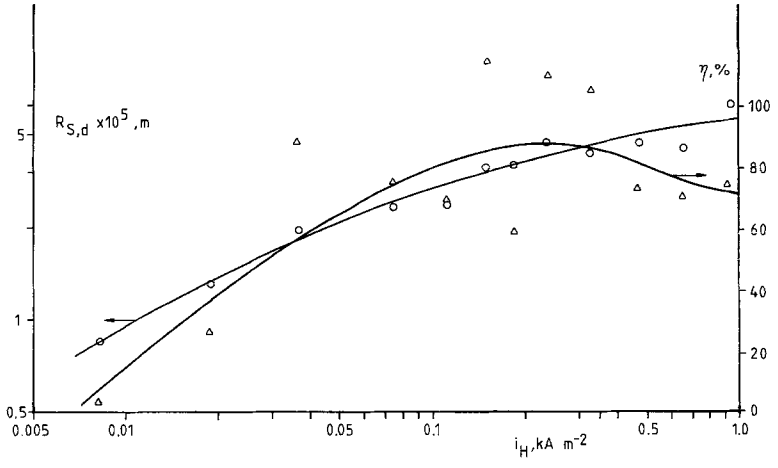

Fig. 2. Sauter bubble radius, $R_{S,d}$, and efficiency of gas bubble formation η, both determined by the high speed film method, as a function of current density for hydrogen evolution on a nickel electrode in 1 M KOH and at 298 K and at a bulk solution flow velocity of 0.12 m s^{-2}.

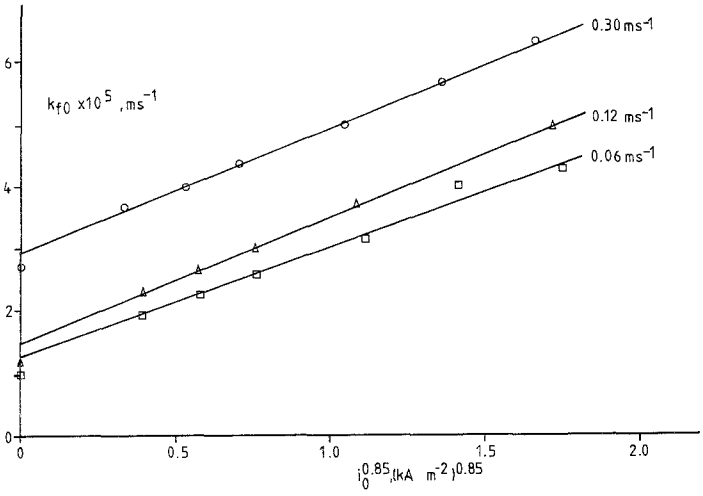

Fig. 3. Mass transfer coefficient for $Fe(CN)_6^{4-}$ to an oxygen-evolving nickel electrode in 1 M KOH and at 298 K and three different bulk solution velocities plotted versus the current density of oxygen evolution.

The mass transfer coefficient $k_{f,fo}$ with forced convection and in the absence of gas evolution was obtained from experiments by measuring the limiting current of $Fe(CN)_6^{4-}$ oxidation at a potential of 450 mV vs SCE and results are given in Fig. 3. This figure shows that $k_{e,fo}$ is larger than $k_{f,fo}$.

3.2.2. Hydrogen-evolving electrode. Fig. 4 shows the mass transfer coefficient k_{fi} as a function of i_H for a hydrogen-evolving electrode in 1 M KOH as the supporting electrolyte, at 298 K and two different flow velocities. The mass transfer coefficient $k_{f,fi}$ was determined by measuring the limiting current at a working electrode potential of -0.5 V. From Fig. 4 it follows that the slight increase in k_{fi} is proportional to i_H. Linear extrapolation of the straight lines of Fig. 4 gives $k_{e,fi}$. Fig. 4 shows that for both velocities of solution flow $k_{e,fi}$ are clearly higher than $k_{f,fi}$. To check the relation between k_{fi} and i_H, represented in Fig. 4, mass transfer experiments were also carried out at up to an i_H of about 10 kA m^{-2}. It was found that $k_{fi} = k_{e,fi} + p_H i_H$ and p_H decreases with increasing i_H.

4. Discussion

It can be argued that the bubble size determined in this investigation is almost equal to that for the bubbles departing from the electrode surface. Obviously, coalescence of attached bubbles can affect the experimental results strongly. It was found that the average radii for oxygen as well as hydrogen detached bubbles are proportional to $i_O^{0.44}$ and $i_O^{0.27}$, respectively.

The oxygen bubbles, formed by coalescence of bubbles which had adhered to the electrode

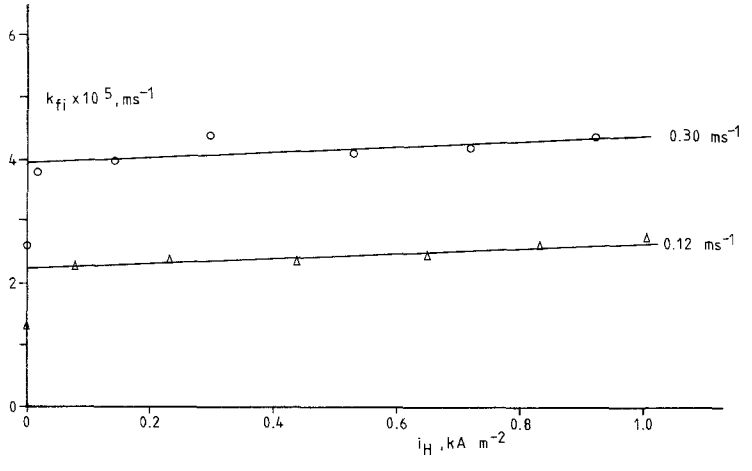

Fig. 4. Mass transfer coefficient for $Fe(CN)_6^{3-}$ to a hydrogen-evolving nickel electrode in 1 M KOH and at 298 K and two different bulk solution flow velocities v_s plotted versus the current density of hydrogen evolution.

surface, jumped perpendicularly from the electrode surface [4].

The density of rising oxygen bubbles in the solution near the electrode surface is relatively low, since no layer of free oxygen bubbles glides over the layer of attached oxygen bubbles [11]. At the hydrogen-evolving electrode bubbles glide over the layer of attached bubbles. It is well known, that in alkaline solution, hydrogen bubbles do not coalesce as easily as oxygen bubbles.

4.1. *Efficiency of gas evolution*

The efficiency of gas evolution is much greater for the hydrogen-evolving electrode than for the oxygen-evolving electrode (Figs. 1 and 2). The calculated efficiency of gas evolution given in [12] is very much less than the experimental results given in Fig. 2. It is likely that the efficiency of gas evolution determined from pictures just above the top of the working electrode is higher than that for the working electrode because of gas absorption by bubbles rising in the supersaturated solution near the gas-evolving electrode. Because of the small height of the working electrode, 5.45 mm, it is likely that the difference in both efficiencies is negligible.

4.2. *Mass transfer at a gas-evolving electrode*

Gas bubble evolution at an electrode causes solution flow near the electrode surface. It is likely that the effect of the solution flow induced by bubbles is reduced with increasing forced convection. Gas bubbles formed at an electrode block the current passage for a part of the electrode surface during their attachment and impede the mass transfer of indicator ions to the electrode surface. After detachment, the space which had been occupied by the detached bubbles is filled by solution. The solution flow needed to fill the space occupied by detached bubbles is considered as a solution flow, the velocity of which has no direct effect on the calculated rate of mass transfer.

From the theoretical description of the convection–migration model it follows that the t_1/t_d ratio is very important. To calculate t_d, the bubble density d has to be used. Unfortunately, this factor is unknown. For the sake of reliability it is assumed that $t_1 < t_d$ at $k < 3k_e$. Consequently, Equation 11 is only used at relatively low values of k, namely $k < 3k_e$.

4.2.1. Oxygen-evolving electrode. From Fig. 1, the factor $D_{fo}A_d v_{g,b}/\pi V_d$ at $v_s = 0.12$ m s^{-1} and at various i_O can be determined considering that $R_{S,d} = 3V_d/4A_d$, $v_{g,b} = \eta_g v_g^0$ and $v_g^0 = i_O V_M/4F$.

Since $V_M = 24.5 \times 10^{-3}$ m^3 it follows that at 298 K $v_g^0 = 0.634 \times 10^{-4} i_O$ m s^{-1} where i_O is given in kA m^{-2}. It has been found that for the oxygen-evolving electrode at $v_s = 0.06$ and 0.12 m s^{-1}, $k_{e,fo}$ is slightly higher than $k_{f,fo}$. This means that the effect of the hydrodynamic convection of solution which occurs at very low current densities, < 0.05 kA m^{-2}, has to be taken into account. To verify the proposed model, $k_{e,fo}$ has to be used.

For an oxygen-evolving electrode the factor $(k_{fo} - k_{e,fo})\,k_{e,fo}$ is plotted versus $D_{fo}A_d v_{g,b}/\pi V_d$ in Fig. 5. The experimental results are scattered around a straight line with a slope $a_{d,O}$ of 1.7. This means that the refreshment mechanism is very effective in enhancing the mass transfer of indicator ions to the surface of an oxygen-evolving electrode. For the oxygen-evolving electrode, the hydrodynamic mechanism is of still less importance in this case, because of the behavior of detaching oxygen bubbles. These bubbles jump perpendicularly from the electrode surface and cause only a weak vertical hydrodynamic

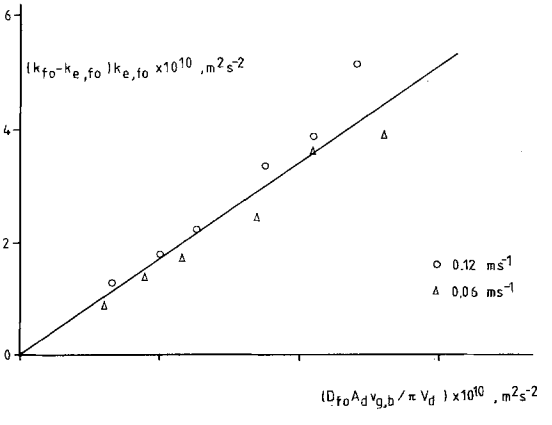

Fig. 5. The factor $(k_{fo} - k_{e,fo})k_{e,fo}$ plotted versus $D_{fo}A_d v_{g,b}/\pi V_d$ for an oxygen-evolving nickel electrode in 1 M KOH and at 298 K and two different bulk solution flow velocities.

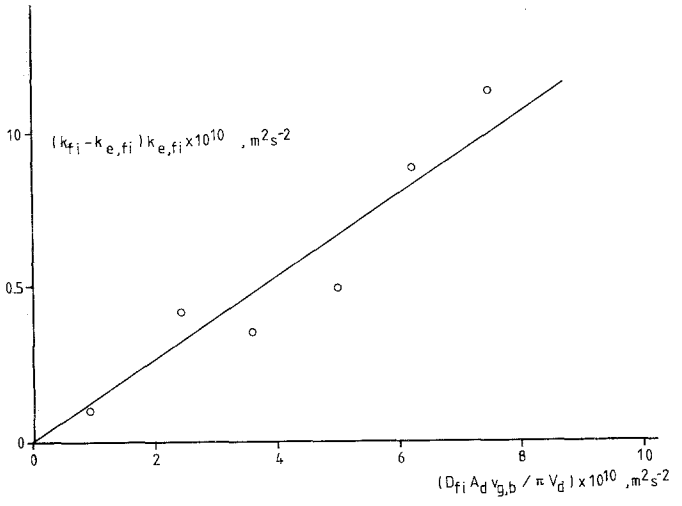

Fig. 6. The factor $(k_{fi}-k_{e,fi})k_{e,fi}$ plotted versus $D_{fi}A_d v_{g,b}/\pi V_d$ for a hydrogen-evolving nickel electrode in 1 M KOH and at 298 K and a bulk solution flow velocity of 0.12 m s^{-1}.

flow of solution near the electrode surface. The detached rising oxygen bubbles do not form a curtain near the electrode surface as the detached rising hydrogen bubbles do.

4.2.2 Hydrogen-evolving electrode. For hydrogen-evolving electrodes it has been found that $k_{e,fi}$ is clearly higher than $k_{f,fi}$ in the investigated range of solution flow velocities. This result can be explained by the formation of a curtain of rising bubbles near the electrode surface and by slipping bubbles attached to the electrode surface. Both phenomena cause a hydrodynamic flow of the solution enhancing the mass transfer near the electrode surface particularly in the range of very low current densities. To elucidate the contribution of the refreshment mechanism to mass transfer it is preferred to use k_e rather than k_f.

In Fig. 6 the difference $k_{fi}k_{e,fi} - k_{e,fi}^2$ is plotted versus $D_{fi}A_d v_{g,b}/\pi V_d$ for a hydrogen-evolving electrode at $v_s = 0.12$ m s^{-1}, where $R_{S,d} = 3V_d/4A_d$ (Fig. 2), $v_{g,b} = \eta_g v_g^0$ where η_g is given in Fig. 2 and v_g^0 at 298 K is 1.268×10^{-4} i_H m s^{-1} where i_H is given in kA m^{-2}. The slope of the straight line drawn in Fig. 6 is equal to $a_{d,H} = 0.14$. This value of $a_{d,H}$ is low and indicates the low effectiveness of the refreshment mechanism for the hydrogen-evolving electrode. If the hydrodynamic mechanism also contributes to the increment of the mass transfer coefficient at $v_s = 0.12$ m s^{-1}, the factor $a_{d,H}$ has then to be smaller than 0.14. In this case, the effectiveness of the refreshment mechanism becomes still lower.

References

[1] H. Vogt in 'Comprehensive Treatise of Electrochemistry' (edited by E. Yeager, J. O.' M. Bockris, B. E. Conway and S. Sarangapani) Vol. 6, Plenum Press, New York, London (1983) p. 445.
[2] N. Ibl, E. Adam, J. Venczel and E. Schalch, *Chem. Ing. Tech.* **43** (1971) 202.
[3] K. Stephan and H. Vogt, *Electrochim. Acta* **24** (1979) 11.
[4] L. J. J. Janssen and S. J. D. van Stralen, *ibid.* **26** (1981) 1011.
[5] L. J. J. Janssen and E. Barendrecht, *ibid.* **24** (1979) 693.
[6] I. Rousar and V. Chezner, *ibid.* **20** (1975) 289.
[7] T. R. Beck, *J. Electrochem. Soc.* **116** (1969) 1038.
[8] H. Vogt, *Electrochim. Acta* **23** (1978) 205.
[9] L. J. J. Janssen and E. Barendrecht, *ibid.*, to be published.
[10] L. J. J. Janssen and J. G. Hoogland, *ibid.* **18** (1973) 543.
[11] L. J. J. Janssen, C. W. M. P. Sillen, E. Barendrecht and S. J. D. van Stralen, *ibid.* **29** (1984) 633.
[12] H. Vogt, Extended Abstracts 34th meeting ISE, Erlangen, 0413, 1983.